support from the Department of Energy (Office of Basic Energy Sciences).

References and Notes

(1) D. M. Ivory, G. G. Miller, J. M. Sowa, L. W. Shacklette, R. R. Chance, and R. H. Baughman, *J. Chem. Phys.*, **71**, 1506 (1979).
(2) F. G. Will, R. S. MacDonald, R. D. Gleim, and M. R. Winkle, *J. Chem. Phys.*, **78**, 5874 (1983).
(3) S. I. Yaniger, S. M. Riseman, T. Frigo, and E. M. Eyring, *J. Chem. Phys.*, **76**, 4298 (1982).
(4) S. I. Yaniger, D. J. Rose, W. P. McKenna, and E. M. Eyring, *Appl. Spectrosc.*, **38**, 7 (1984).
(5) D. W. Vidrine, *Appl. Spectrosc.*, **34**, 314 (1980).
(6) G. Wegner, *Angew. Chem., Int. Ed. Engl.*, **20**, 361 (1981), and references contained therein.
(7) P. Kovacic and J. Oziomek, *J. Org. Chem.*, **29**, 100 (1964), and references contained therein.
(8) T. Yamamoto and A. Yamamoto, *Chem. Lett.*, 353 (1977), and references contained therein.
(9) S. M. Riseman, F. E. Massoth, G. M. Dhar, and E. M. Eyring, *J. Phys. Chem.*, **86**, 1760 (1982).
(10) G. Froyer, F. Maurice, P. Bernier, and P. McAndrew, *Polymer*, **23**, 1103 (1982).
(11) C. F. Hsing, I. Khoury, M. D. Bezoari, and P. Kovacic, *J. Polym. Sci., Polym. Chem. Ed.*, **20**, 3313 (1982).
(12) L. W. Shacklette, H. Eckhar R. Chance, G. G. Miller, D. M. Ivory, and R. H. Baughr *J. Chem. Phys.*, **73**, 4098 (1980).
(13) S. Krichene, S. Lefrant, G. Froyer, F. Maurice, and Y. Pelous, *J. Phys. (Paris)*, **44**, 733 (1983).
(14) S. Yaniger, W. S. Huang, and A. G. MacDiarmid, unpublished results.
(15) J. P. Collman and L. S. Hegedus, "Principles and Applications of Organotransition Metal Chemistry", University Science Books, Mill Valley, CA, 1980.
(16) S. I. Yaniger, W. P. McKenna, E. M. Eyring, and W. Woolfenden, unpublished results.
(17) J. F. Liebman, private communication.

Molecular Order in Condensed States of Semiflexible Poly(amic acid) and Polyimide

Nobuyuki Takahashi,† Do Y. Yoon,* and William Parrish

IBM Research Laboratory, San Jose, California 95193. *Received April 10, 1984*

ABSTRACT: The molecular order in condensed states of the aromatic poly(amic acid) (PAA) poly(4,4′-oxydiphenylenepyromellitamic acid) and the resulting polyimide (PI) poly(4,4′-oxydiphenylenepyromellitimide) obtained by heating PAA films was determined from wide-angle X-ray diffraction studies. PAA chains in films containing solvents of ~30% by weight exhibit parallel alignment and correlated (smectic-like) lateral packing of highly extended chain segments, as shown by the appearance of a diffraction peak due to the intramolecular periodicity of ~14 Å. Upon imidization and removal of solvents by heating at 200 °C, this molecular order is preserved and slightly improved in the resulting PI films. Further improvement in order occurs upon annealing PI films at temperatures above ca. 300 °C, with the details of changes depending strongly on the initial orientation. In all PI samples, however, the high-angle diffraction patterns in the region of the scattering vector s ($=(2 \sin\theta)/\lambda$) > 0.35 Å^{-1} are matched very closely by the theoretical curve calculated for a single repeat unit, thereby indicating the absence of any appreciable long-range crystalline order in the thermally imidized PI films. The ramifications of such molecular order in condensed states of PAA (which cannot crystallize due to the meta–para isomers in the pyromellitamic acid unit) and PI are discussed in light of recent theoretical developments in the statistical thermodynamics of semiflexible polymers as well as some unique characteristics exhibited by this polyimide.

Introduction

The polymers comprising planar rigid groups interconnected to each other with fixed bond angles (i.e., aromatic polyimides, polysulfones, polycarbonates, etc.) normally exhibit a combination of high softening temperatures, thermal stability, and tough mechanical properties and thus are highly desirable for various demanding technological applications. On the molecular level, inclusion of such long rigid groups in the polymer backbone reduces the chain "flexibility", as demonstrated by detailed investigations[1,2] of their unperturbed chain configurations in dilute solutions devoid of excluded volume effect. For polymers with sufficient flexibility, the *unperturbed random coil* configuration is directly applicable to the chains in concentrated solutions and in the bulk.[3] However, this relationship cannot hold for polymers with limited flexibility as shown by theoretical considerations of semiflexible polymers in condensed states.[4-7] These considerations lead to the prediction that, for polymers with insufficient flexibility, an ordered state exhibiting both orientational and conformational order can be more stable than the isotropic state of random chains. Furthermore, the degree of order in conformation and orientation in the ordered state depends strongly on the chain model. Hence, the decreased chain flexibility due to the presence of planar cyclic groups of considerable length in the chain backbone poses a rather important question concerning the chain configurations, or molecular order, of these polymers in condensed states.

In this paper, we examine the molecular order of the aromatic poly(amic acid) (PAA) poly(4,4′-oxydiphenylenepyromellitamic acid) and the corresponding polyimide (PI) poly(4,4′-oxydiphenylenepyromellitimide) obtained by thermal imidization of PAA films,[8] shown schematically in Figure 1. The PAA chain comprises rigid groups of ca. 18 and 9 Å in length for the para and meta linkages of the pyromellitamic unit,[2], respectively, distributed randomly along the chain[9] and due to this structural irregularity cannot crystallize. The PI chain comprises rigid groups of ca. 18 Å in length[2] and is known to exhibit crystallinity upon heating the highly drawn fibers or films.[10-12] The structure of PAA films has received very little attention. While the structure in PI films or fibers has been the subject of a rather large number of studies,[10-14] most of the attention has been focused on the issues of crystallinity, crystal structure, and crystalline aggregates, etc. The structures or molecular order in

† IBM World Trade Postdoctoral Fellow. Permanent address: Department of Physics, Hokkaido University of Education, Hakodate, 040, Japan.

0024-9297/84/2217-2583$01.50/0 © 1984 American Chemical Society

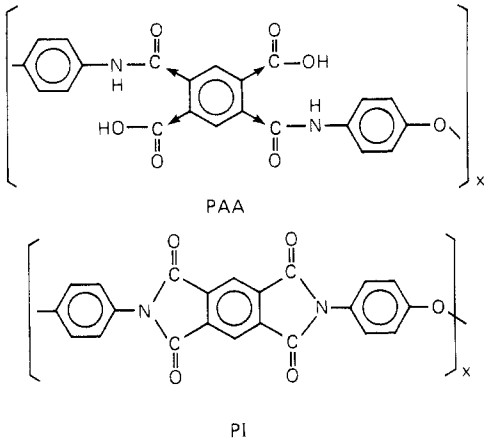

Figure 1. Schematic diagram of the repeat unit of poly(4,4'-oxydiphenylenepyromellitamic acid) (PAA) and poly(4,4'-oxydiphenylenepyromellitimide) (PI).

noncrystalline states of PAA and PI have not been investigated, despite their ramifications concerning the statistical thermodynamics of semiflexible polymers as well as the technological importance of this class of polymers,[8] which includes applications in microelectronic devices.[15]

Experimental Section

Materials. PAA of $M_w \sim 28000$ was obtained from Du Pont Corp. in concentrated solutions of ~18% by weight in *N*-methylpyrrolidone and xylene (4:1). PAA films, ~100 μm in thickness, were prepared by coating the solutions on glass substrates by doctor blading, followed by drying at 100 °C for 30 min. The solid films, which contain solvents of ~30% by weight,[8] were then taken off the substrates. The oriented PI films were prepared by spin-coating PAA solutions on glass substrates at ~300-rpm spin speed, drying at 100 °C for 30 min, and heating at 200 °C for 1 h in a nitrogen atmosphere before removing from the substrate. The curing condition was adopted in view of previous studies which showed that PAA in condensed states undergoes a rather rapid imidization above ~150 °C[8] and imidization is nearly completed by heating PAA films at ~200 °C for ~1 h.[16,17] The average thickness of oriented PI films was ca. 7 μm. Unoriented PI films were obtained by removing PAA films from the substrates and heating at 200 °C for 3 h in a nitrogen atmosphere. Annealed PI films, both oriented and unoriented, were prepared by heating the PI films described above at a preset temperature for 2 h in a free-standing form in a nitrogen atmosphere; four different temperatures of 250, 300, 350, and 400 °C were employed in this study.

A single flat layer of film, mounted on aluminum rings, was used for X-ray measurements of PAA and unoriented PI samples, while a stack of 10 films was used for oriented PI samples. The area exposed to the X-ray beam was not supported to avoid extraneous background.

X-ray Measurements. The experimental runs were automated with an IBM Series/1 minicomputer.[18] The following X-ray parameters were used with vertical plane focusing diffractometers:[19] long fine-focus Cu target X-ray tube operated at 50 kV and 20 mA with a 12° take-off angle, goniometer radius R = 185 mm, various angular apertures determined by the divergence slit widths (see below), incident beam parallel foil collimator aperture 4.5° (none in diffracted beam), receiving slit 0.11° (0.35 mm), vacuum specimen chamber and X-ray path to eliminate air scatter, and NaI–Tl scintillation counter with single-channel pulse amplitude discrimination. Most of the runs were made with reflection geometry and curved pyrolytic graphite monochromator set for Cu Kα radiation in the diffracted beam.

The transmission runs used an asymmetric cut 10.1 quartz crystal monochromator bent to a section of a logarithmic spiral.[19] In both reflection and transmission geometries, the specimen was continually rotated (77 rpm) around an axis normal to the surface of the specimen. Careful alignment of the beam and antiscatter slits was required to avoid false scattering at the small diffraction angles.

Table I
Typical Experimental Parameters[a]

2θ range, deg	Δ2θ, deg	t, s	DS, deg	highest count rate, counts s^{-1}
3–10	0.2	50	0.25	764
9–24	0.2	30	0.50	1002
20–43	0.5	30	1.00	794
39–80	1.0	50	2.00	129
76–110	1.0	50	4.00	29
110–160	2.0	50	4.00	17

[a] These are the set of parameters used to obtain the results of Figure 2.

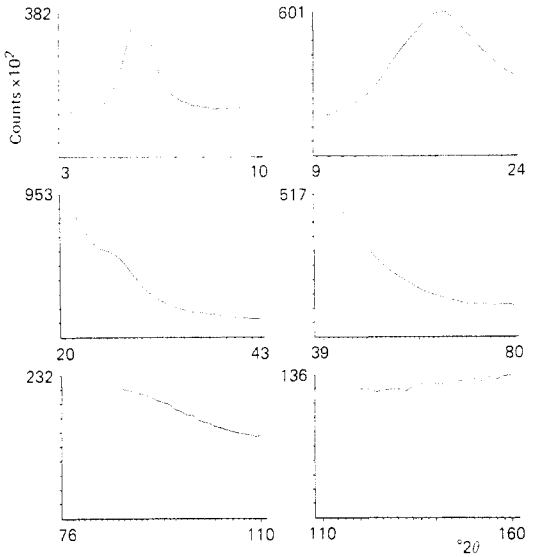

Figure 2. Computer displays of experimental data showing six segments of a typical run taken for the unoriented PI annealed at 350 °C using the parameters listed in Table I.

A large number of preliminary runs were made to determine the optimum experimental conditions. A typical experimental run took about 4 h. Each run was programed in six angular range segments to use the best experimental conditions in each segment as shown in Table I. The maximum divergence slit aperture DS was selected to correspond to the minimum 2θ angle in each segment in order to obtain the highest intensity and to prevent the X-ray beam from exceeding the 25-mm specimen diameter. Each range overlapped a few degrees to determine the scaling factors. The angular increments in the step scanning, Δ2θ, were selected as large as possible to be consistent with the required resolution and minimum experimental time. The 30- or 50-s count time t per step was determined from the approximate "average" intensity in that segment. The intensities in the high-angle regions were very low and would have required nearly an hour per step to accumulate the same number of counts in the forward reflection segments and t = 50 s was selected as a practical value. The last column lists the highest intensity in counts per second in each segment normalized for t and DS. Figure 2 shows the computer displays of a typical run using the complete set of experimental parameters listed in Table I, taken for unoriented PI films annealed at 350 °C.

In the forward reflection region, the coherent Cu Kα scattering and the incoherent scattering (Compton modified) are overlapped and the experimental data include both. They become increasingly separated as the diffraction angle 2θ increases, and the intensity of the incoherent scattering increases and becomes larger than the coherent radiation at large 2θ. The diffracted beam monochromator reflects only the Cu Kα radiation and an increasing portion of the incoherent scattering is not recorded with increasing 2θ, causing a systematic error in the experimental intensities. Because some assumptions must be made in calculating the error, a separate set of experiments was made to accurately account for the coherent and incoherent scattering at high 2θ. These measurements were made with an energy-dispersive diffractometer using a Si(Li) detector and multichannel

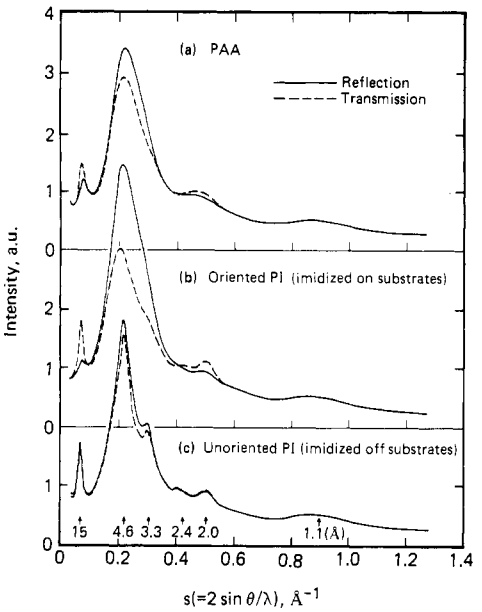

Figure 3. X-ray diffraction patterns obtained from the reflection (solid line) and transmission (dashed line) diffractometry for (a) PAA, (b) oriented PI, and (c) unoriented PI. The lattice spacings corresponding to the scattering vectors where unoriented PI exhibits diffraction maxima are indicated along the horizontal abscissa.

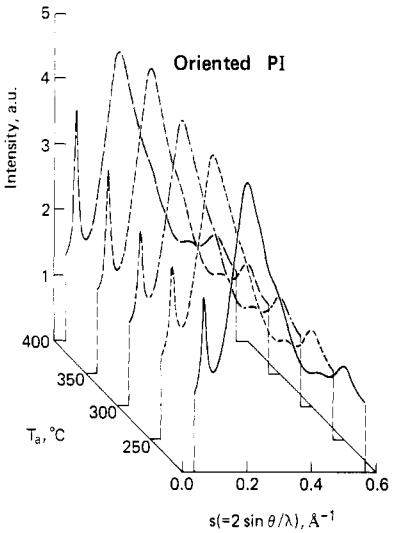

Figure 4. X-ray diffraction patterns in transmission obtained for oriented PI films annealed at the temperatures denoted by T_a. The profile of the initial oriented PI is also shown (solid line) for comparison.

analyzer without monochromator.[20] Even at 160° 2θ, the coherent scattering and incoherent scattering were not completely resolved. These runs were also computer automated and required 15–20 h each because of the low intensities.

Results

After the measured X-ray intensities were corrected for absorption and polarization, the scale of intensities was adjusted for different samples by matching the intensity at 52° (2θ) for the transmission profiles and by matching the integrated intensity over the interval 52–160° (2θ) for the reflection profiles, respectively. These results were then converted to plots of intensity (counts) vs. the scattering vector s (=(2 sin θ)/λ), equal to the reciprocal of the d spacing, and are shown in Figures 3–6.

PAA. The X-ray diffraction patterns of PAA films are shown in Figure 3a. The differences between the reflection and the transmission patterns indicate the preferred orientation of PAA chains along the film plane.[17] The first peak has a d spacing of 13.9 Å in transmission and 13.2 Å in reflection. This periodicity of 13–14 Å arises from the repeat distances along the molecular chain, since its intensity is stronger in the transmission geometry in which the scattering vector coincides with the direction of the preferred orientation of PAA chains.

This peak is 2.4° (2θ) wide at half peak height above background. Using the Scherrer equation and the instrument broadening function of 0.14° (2θ) at this 2θ angle gives a coherence length of 37 Å. One-dimensional or planar order in the molecular packing is unlikely because there is no appreciable asymmetry in the profile of this diffraction peak. At higher angles, only broad halos typical of amorphous polymers occurred.

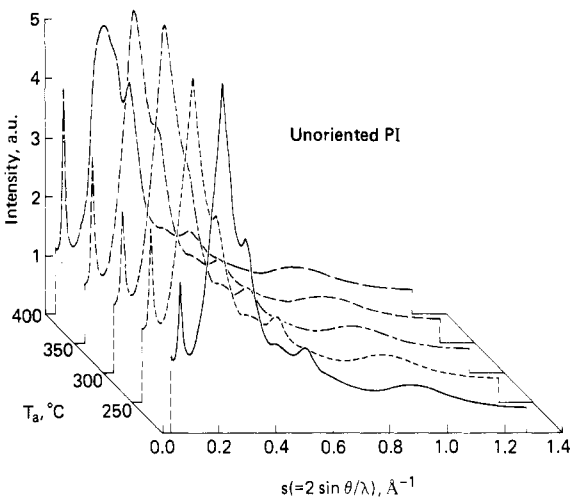

Figure 5. X-ray diffraction patterns in reflection obtained for unoriented PI films annealed at the temperatures denoted by T_a. The profile of the initial unoriented PI is also shown (solid line) for comparison.

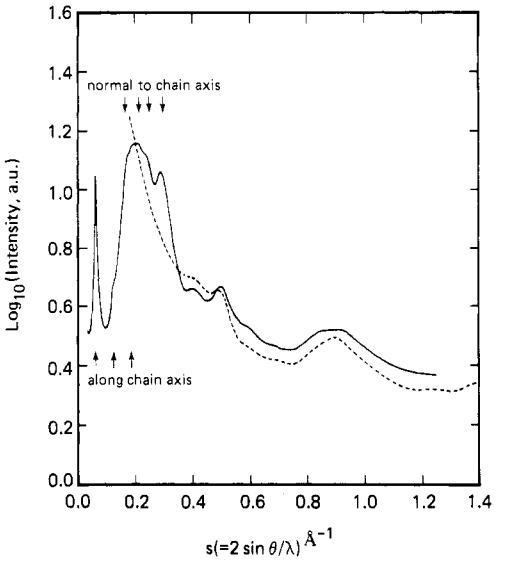

Figure 6. Comparison of the X-ray diffraction patterns of unoriented PI with the structure factor of the PI repeat unit. The experimental profile (solid line) in the region of $s < 0.35$ Å^{-1} denotes the data of unoriented PI annealed at 400 °C, obtained by the diffracted beam monochromator system. In the region of $s > 0.35$ Å^{-1} the experimental profile (identical for all unoriented PI samples regardless of annealing temperatures) was obtained with an energy-dispersive solid-state detector system to account for both the coherent and the incoherent scattering. The theoretical curve (dotted line) also includes both the coherent and the incoherent scattering and is matched to the experimental pattern at $s = 0.35$ Å^{-1}; see text.

This result indicates that PAA chains in condensed states assume a highly ordered structure. Since the PAA chain contains the para- and meta-isomeric linkages in the pyromellitamic acid unit (see Figure 1), probably with equal chance,[9] the possibility of crystallinity as the source of this ordered structure can be eliminated. The absence of any periodicity perpendicular to the chain axis further confirms this conclusion.

The observed repeat distance of 13–14 Å is close to the projected length of the monomer unit along the axis of the fully extended chain which is estimated to be 15.9 Å for both the para- and meta-pyromellitamic linkages.[2] Hence, our results suggest that PAA chains in condensed states assume nearly fully extended local conformations. Furthermore, neighboring chains pack with one another in such a manner that the positions of monomer units of a given chain along the extended chain axis are in register with those of the neighboring chains, its coherence persisting over the span of ca. 37 Å. Along the lateral directions, however, no periodicity is assumed. In essence, this order may be likened to that of smectic liquid crystals.

Oriented PI. The diffraction patterns of PI films prepared by thermal imidization of PAA on substrates are shown in Figure 3b. They have much more pronounced chain orientation than the PAA films, but other than this orientation effect, the overall diffraction patterns are very similar to those of PAA. The lowest angle peak has a spacing of 14.5 Å, somewhat larger than that of PAA. Also, this reflection is somewhat sharper than that of PAA; the coherence length determined from its half-width is increased to 55 Å. This diffraction peak is again due to the repeat periodicity along the PI chain axis, as demonstrated by previous X-ray studies on highly stretched PI fibers and films.[10-13] The periodicity of 14.5 Å is close to the value of 15.4 Å, the repeat unit spacing along the axis of the fully extended chain.[2] The three higher angle halos are also very similar to those of PAA and, hence, indicate the absence of crystallinity.

The molecular order in oriented PI films therefore appears to be very close to that of PAA films, with PI chains assuming fully extended local conformations. The somewhat improved order as shown by the sharper low-angle peak may be due to the regularity in the chemical bonding of the PI chain (i.e., absence of meta–para isomers) as well as the removal of residual solvents. The integrated intensity of the low-angle peak averaged over the reflection and transmission experiments is ~20% lower than that of PAA; however, considering the uncertainty involved in accounting for the orientation effect, this difference is within the experimental errors. Hence, the molecular order in PAA films seems mostly preserved in oriented PI films prepared by thermal imidization on substrates.

Unoriented PI. The diffraction patterns from the PI films prepared by thermal imidization of PAA films in a free-standing form are shown in Figure 3c. The transmission and the reflection patterns match very closely, indicating a significant reduction in chain orientation during thermal imidization of (oriented) PAA films in a free-standing condition.[17] The low-angle peak has a spacing of 15.0 Å and the coherence length is ca. 64 Å. The first halo (over s = 0.13–0.35 Å^{-1}) exhibits more fine structure than that of the oriented PI, whereas the second halo (over s = 0.35–0.65 Å^{-1}) is virtually identical with that of the transmission profile of oriented PI. The PI chains in unoriented films therefore seem to have a slightly better order along the chain axis as well as along the lateral direction, compared to those of oriented PI and PAA. However, the integrated intensity of the low-angle reflection of unoriented PI is almost identical with that of PAA and, hence, the overall molecular order in unoriented PI films does not seem to differ significantly from that of the "smectic-like" order in PAA films and in oriented PI films.

Table II
Change in the Low-Angle Peak of Unoriented PI with Annealing

anneal temp, °C	d spacing, Å	coherence length, Å	I(peak) − I(bkgd) au	[I(peak) − I(bkgd)]/ I(bkgd)
init sample	15.0	64	335	1.1
250	15.2	71	415	1.4
300	14.8	65	385	1.3
350	15.5	74	522	2.1
400	15.6	74	659	3.4

Structural Changes by Annealing. The transmission patterns of the annealed oriented PI films prepared by heating the initial oriented PI films at the temperatures of 250, 300, 350, and 400 °C, respectively, are shown in Figure 4. No appreciable changes are observed over the entire range of scattering vectors up to 300 °C. The initial change occurs at 350 °C, which causes increased intensity of the low-angle peak. A further intensity increase of this peak is observed at 400 °C; the total integrated intensity under this peak is increased by ~30% and its width is decreased by ~20%, compared with that of the initial oriented PI. At higher scattering vectors, however, no change is observed at all annealing temperatures. Therefore, it seems that although the initial molecular order in oriented PI films can be improved somewhat by annealing at temperatures higher than ~350 °C, no major departures from the initial order in PAA films occur regardless of annealing temperatures.

Unoriented PI films, imidized initially in a free-standing form, exhibit more significant structural changes upon annealing, as shown by the reflection patterns in Figure 5. The low-angle reflection undergoes a major increase in its intensity at 350 °C and becomes more intense at 400 °C, similar to the situation of oriented PI films (see Figure 4). As the detailed analyses listed in Table II show, the d spacing also increases significantly at 350 °C. These results also indicate a decrease in order at 300 °C from that at 250 °C, as shown by the changes in d spacing, coherence length, and peak intensity. The broad peaks at 4.6- and 3.3-Å spacings (see Figure 2c) also become broader by annealing at 300 °C, indicating decreased order in the lateral chain packing. The 3.3-Å peak starts to sharpen at 350 °C and gets sharper at 400 °C. Annealing at 400 °C also produces five bumps around the initial 4.6-Å peak as shown in more detail in Figure 6; three of these five bumps correspond to the (equatorial) reflections observed by Conte et al.[12] in the direction normal to the chain axis for the highly stretched PI films, and the remaining two correspond to the second- and the third-order reflections of the low-angle peak. This indicates that the molecular packing in unoriented PI films improves and begin to exhibit some crystalline features at 400 °C. The scattering vectors $s > 0.35$ Å^{-1}, however, show no appreciable changes at all annealing temperatures. Furthermore, the diffraction profiles in this range are very close to those of oriented PI in the transmission geometry. Actually, the diffraction profiles in this range of scattering vectors are changed only by the initial imidization of PAA to PI, suggesting that they may represent the structure factor of the PI repeat unit itself.

Scattering Function of the PI Repeat Unit. To determine whether the diffraction patterns in the range of scattering vectors $s > 0.35$ Å^{-1} are due entirely to the

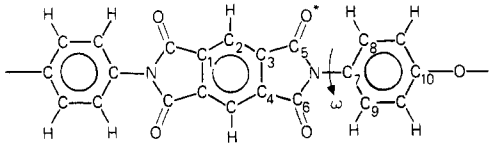

Figure 7. Schematic diagram of the PI repeat unit denoting various atoms designated in Table III.

Table III
Bond Geometry of PI Repeat Unit[a]

bond angle, deg		bond length, Å	
C_1–C_2–C_3	117.0	C_2–C_3	1.396
C_4–C_3–C_5	108.5	C_3–C_4	1.394
C_3–C_5–N	105.9	C_3–C_5	1.480
C_5–N–C_6	111.2	C_5–O*	1.203
N–C_5–O*	124.3	C_5–N	1.414
C_8–C_7–C_9	120.0	N–C_7	1.428
		C_7–C_8	1.395
		C_{10}–O	1.390
		C^{ar}–H	1.08

[a] All geometrical parameters are taken as the averages of equivalent geometries in the crystal structure of 4,4′-bis(phthalimide) diphenyl ether obtained in ref 21.

structure factor of the repeat unit of the PI chain, the scattering function of the repeat unit was computed from the known geometrical parameters. Both the coherent and the incoherent scattering contributions are included in the theoretical scattering function, calculated by employing the bond lengths and the bond angles denoted in Figure 7 and Table III. The torsional angle ω between the plane of pyromellitimide and that of the oxyphenylene was taken to be 60° from the crystal structure of 4,4′-bis(phthalimide) diphenyl ether.[21] This theoretical profile, shown by the dotted line in Figure 6, matches closely the experimental curve obtained with an energy-dispersive solid-state detector to include both the coherent and the incoherent scattering intensities in the region $s \geq 0.35$ Å^{-1}; the experimental curve for $s < 0.35$ Å^{-1} was obtained by using the diffracted beam monochromator system and the intensities by the two methods as well as the theoretical curve were matched at $s = 0.35$ Å^{-1}. The close agreement in the region $s > 0.35$ Å^{-1} between the experimental pattern and the theoretical curve calculated for a single repeat unit shows that the diffraction profile in this region indeed reflects mainly the chemical structure of PI and thus confirms the absence of any significant crystalline order in all PI films investigated in this study.

Discussion

The results presented above show that PAA chains in condensed states exhibit a high molecular order resembling that of a smectic liquid crystalline state and, furthermore, this order is virtually preserved and somewhat improved upon thermal imidization to form PI films. The molecular chains assume nearly fully extended local conformations in both PAA and PI films. While a significant improvement in chain packing can be obtained by annealing unoriented PI films at high temperatures close to 400 °C, no indication of any appreciable crystalline order is found in the thermally imidized PI films.

The fact that PAA chains in the normally prepared films exhibit an ordered state of extended chains seems to provide a logical explanation for the observation that the imidization reaction, often called curing, is virtually completed at 200 °C,[16] which is substantially below the glass transition temperature of this PI chain believed to be above 300 °C.[8] This implies that imidization can occur without requiring a substantial rearrangement of spatial configurations of the PAA chains. Our results are consistent with this observation.

The results on annealing effects are relevant to the discussions concerning the glass transition temperature, or softening point, of this polyimide. Both the oriented PI and the unoriented PI show that a significant increase in molecular odering along the chain axis begins to occur between 300 and 350 °C. This is consistent with the conclusions of Barton and Critchley,[22] who showed that the initial glass transition temperature of this PI is ca. 325 °C from the extrapolation of the DSC results of copolymers. It is further corroborated by our dielectric relaxation and thermal expansion measurements[23] on the *unconstrained*[24] films of this polyimide. However, as the molecular order undergoes changes above this temperature, attaining better order with increasing temperature, the softening point will keep changing when the PI samples are exposed to higher temperatures, and hence this initial softening temperature is observed only during the first heating process.[23]

The observation that PAA chains assume a high molecular order in condensed states needs to be related to the configurational characteristics of PAA. Following the procedure described by Birshtein,[2] but employing the phenylene–oxygen–phenylene angle of 118°[21] instead of 120°, the ratio of the mean-square end-to-end chain vector to the fully extended chain length, $\langle r^2 \rangle / L$, is estimated to be ca. 59 Å for the para linkage of the pyromellitamic group and ca. 31Å for the meta linkage *at all temperatures*. This ratio corresponds to the Kuhn length L_K in the equivalent freely jointed chain model.[25] The mean diameter D of the PAA chain estimated from $D^2L = M/\rho N_A$ (where M is the molecular weight, ρ is the density, and N_A is Avogadro's number) is approximately 5.7 Å, taking the density to be ~1.4.[26] Hence, the mean axial ratio L_K/D of the Kuhn length for the equivalent freely jointed chain becomes ~7.9. This exceeds the critical value of $L_K/D \sim 6.4$, beyond which the ordered state is predicted to be stable at all temperatures for the freely jointed chains in the bulk.[5] Alternatively, in terms of the wormlike chain model with limiting curvature (WCLC) developed recently,[27] the ratio of $\langle r^2 \rangle / L$ at infinite temperature corresponds to the cutoff wavelength L_c, representative of the maximum allowed curvature at all temperatures. The critical axial ratio of the cutoff wavelength L_c required for the absolute stability of an ordered state in the bulk is predicted to be ca. 4.45 in the limit of high molecular weights.[6] The value of $L_c/D \sim 7.9$ estimated for the PAA chain is thus well above this critical value. Therefore, the occurrence of an ordered state in condensed states of PAA is consistent with the predictions of the theories based on the freely jointed chain model or the WCLC model, even though neither of these models can be considered satisfactory in representing the detailed configurational characteristics of PAA.

Finally, it is of interest to note that the corresponding value of L_K/D or L_c/D for the polycarbonate of diphenylol-2,2′-propane is estimated to be ~4.3, from the recent investigations of its geometry and unperturbed chain configurations[28] and its density of 1.2.[29] The fact that this polycarbonate chain assumes random coil configurations in the amorphous state[28,30,31] is also consistent with the theoretical predictions discussed above. This consideration suggests further investigations on the molcular order vs. chemical structure for other polymers comprising planar cyclic groups interconnected with fixed bond angles, in order to better define the boundary of disorder–order transition of this type of semiflexible polymers.

Acknowledgment. We thank D. Quilichi and R. Diller

for preparing the sample and acknowledge helpful discussions with Drs. T. Russell and P. Cotts concerning sample preparation and characterization. Dr. M. Mantler, visiting scientist from Vienna Technical University, made the energy-dispersive X-ray measurements and G. S. Lim aided in the diffractometer runs. N. Takahashi thanks IBM World Trade of Japan for providing a postdoctoral fellowship.

References and Notes

(1) Williams, A. D.; Flory, P. J. *J. Polym. Sci., Part A-2* **1968**, *6*, 1945.
(2) Birshtein, T. M. *Vysokomol. Soedin., Ser. A* **1977**, *16*, 54 [*Polym. Sci. USSR (Engl. Transl.)* **1977**, *19*, 63.]
(3) Flory, P. J. *Faraday Dicuss. Chem. Soc.* **1979**, *68*, 14 and references therein.
(4) Flory, P. J. *Proc. R. Soc. London, Ser. A* **1956**, *234*, 73; *Proc. Natl. Acad. Sci. U.S.A.* **1982**, *79*, 4510.
(5) Flory, P. J. *Macromolecules* **1978**, *11*, 1141. Flory, P. J.; Ronca, G. *Mol. Cryst. Liq. Cryst.* **1979**, *54*, 289.
(6) Ronca, G.; Yoon, D. Y. *J. Chem. Phys.* **1982**, *76*, 3295.
(7) Yoon, D. Y.; Baumgärtner, A. *Macromolecules*, in press.
(8) Sroog, C. E. *J. Polym. Sci., Macromol. Rev.* **1976**, *11*, 161.
(9) Denisov, V. M.; Svetlichnyi, V. M.; Gindin, V. A.; Zubkov, V. A.; Kol'tsov, A. I.; Koton, M. M.; Kudryavtsev, V. V. *Vysokomol. Soedin., Ser. A* **1979**, *21*, 1498 [*Polym. Sci. USSR (Engl. Transl.)* **1979**, *21*, 1644.]
(10) Ikeda, R. M. *Polym. Lett.* **1966**, *4*, 353.
(11) Kazaryan, L. G.; Tsvankin, D. Ya.; Ginzburg, B. M.; Tuichiev, Sh.; Korzhavin, L. N.; Frenkel, S. Ya. *Vysokomol. Soedin., Ser. A* **1972**, *14*, 1199 [*Polym. Sci. USSR (Engl. Transl.)* **1972**, *14*, 1344.]
(12) Conte, G.; D'Illario, L.; Pavel, N. V.; Giglio, E. *J. Polym. Sci., Polym. Phys. Ed.* **1976**, *14*, 1553.
(13) Isoda, S.; Shimada, H.; Kochi, M.; Kambe, H. *J. Polym. Sci., Polym. Phys. Ed* **1981**, *19*, 1293.
(14) Russel, T. P. *J. Polym. Sci., Polym. Phys. Ed* **1984**, *22*, 1105.
(15) Larson, R. A. *IBM J. Res. Dev.* **1980**, *24* (3), 268.
(16) Baise, A.; Buchwalter, L. P., private communication.
(17) Russel, T. P.; Gugger, H.; Swalen, J. D. *J. Polym. Sci., Polym. Phys. Ed.* **1983**, *21*, 1745.
(18) Parrish, W.; Ayers, G. L.; Huang, T. C. *Adv. X-Ray Anal.* **1980**, *23*, 313; IBM Research Report RJ-3524, 1982.
(19) Parrish, W. "X-Ray Analysis Papers"; Centrex Publishing Co.: Eindhoven, 1965.
(20) Mantler, M.; Parrish, W. *Adv. X-Ray Anal.* **1977**, *20*, 171.
(21) Hupfer, B.; Krohnke, C.; Yoon, D. Y., in preparation.
(22) Barton, J. M.; Critchley, J. P. *Polymer* **1970**, *11* (4), 212.
(23) Destruel, P.; Yoon, D. Y., in preparation.
(24) This applies only to the films in a free-standing form; constrained films, e.g., coatings on substrates, do not show the same characteristics.[23]
(25) Kuhn, W. *Kolloid-Z.* **1936**, *76*, 258; **1939**, *87*, 3.
(26) Russell, T. P., private communication.
(27) Ronca, G.; Yoon, D. Y. *J. Chem. Phys.* **1984**, *80*, 930.
(28) Yoon, D. Y.; Flory, P. J. *Polym. Bull.* **1981**, *4*, 693.
(29) Morgan, R. J.; O'Neal, J. E. *J. Polym. Sci., Polym. Phys. Ed.* **1976**, *14*, 1053.
(30) Gawrish, W.; Brereton, M. G.; Fischer, E. W. *Polym. Bull.* **1981**, *4*, 687.
(31) Ballard, D. G. H.; Burgess, A. N.; Cheshire, P.; Janke, E. W.; Niven, A.; Schelten, J. *Polymer* **1981**, *22*, 1353.

Lignin. 20. Associative Interactions between Kraft Lignin Components†

Simo Sarkanen

Department of Chemical Engineering, University of Washington, Seattle, Washington 98195, and Department of Forest Products, University of Minnesota, St. Paul, Minnesota 55108

David C. Teller

Department of Biochemistry, University of Washington, Seattle, Washington 98195

Clyde R. Stevens and Joseph L. McCarthy*

Department of Chemical Engineering, University of Washington, Seattle, Washington 98195. *Received December 21, 1983*

ABSTRACT: The profiles described by eluting gymnosperm kraft lignins from dextran gels with 0.10 M aqueous NaOH represent effective molecular weight distributions that approach those for the discrete components. Under aqueous conditions between pH 13 and 14, dissociation of kraft lignin complexes occurs in dilute solution ($\sim$0.5 g L^{-1}), while a marked tendency for kraft lignin components to associate prevails at higher concentrations ($\sim$20–150 g L^{-1}). These processes are, furthermore, reversible. The apparent molecular weight distributions of kraft lignins are affected by the presence of counterions and zwitterions in alkaline solution and are remarkably sensitive to the method employed for their isolation. The relative ratios of kraft lignin components with molecular weights below 3500 do not, however, vary with the degree of association for the sample as a whole. The relationship between the overall weight-average and number-average molecular weights indicates that the ensemble average product of the molecular weights of interacting species remains constant during association in aqueous alkaline solution. This implies that the associative processes occurring within kraft lignin samples are stoichiometrically constrained: each of the associated complexes possesses a locus which is respectively complementary to only one type of component.

Introduction

The first exploratory investigation revealing that lignin components tend to associate with one another was published 20 years ago.[1] However, the appearance three years later of a second article[2] demonstrating the existence of such phenomena prompted no further studies of the effect for more than a decade. Thus the field of lignin chemistry was beset by a conceptual deficiency at a relatively fundamental level: reliable methods for determining the molecular weight distributions of lignin samples were only recognized quite recently.[3]

In solutions without dissolved electrolytes, the apparent molecular weight distributions of gymnosperm kraft lignins

† All experimental work was conducted at the University of Washington. The analysis of the results was developed by S.S. after transferring to his present position at the University of Minnesota, where the paper was also mainly written.

0024-9297/84/2217-2588$01.50/0 © 1984 American Chemical Society